Science of the Total Environment 828 (2022) 154490

Contents lists available at ScienceDirect

Science of the Total Environment

journal homepage: www.elsevier.com/locate/scitotenv

Morphochemical investigation on the enrichment and transformation of hazardous elements in ash from waste incineration plants

Muhammad Ubaid Ali [a], Yuan Liu [b,*], Balal Yousaf [b], Ming Hung Wong [c], Ping Li [a], Guijian Liu [b], Ruwei Wang [d], Yong Wei [b], Muyuan Lu [b]

[a] State Key Laboratory of Environmental Geochemistry, Institute of Geochemistry, Chinese Academy of Sciences, Guiyang 550081, Guizhou, China
[b] CAS Key Laboratory of Crust-Mantle Materials and the Environments, School of Earth and Space Sciences, University of Science and Technology of China, Hefei 230026, Anhui, China
[c] Consortium on Health, Environment, Education and Research (CHEER), Department of Science and Environmental Studies, The Education University of Hong Kong, Hong Kong, China
[d] School of Environment, Jinan University, Guangzhou 511443, Guangdong, China

HIGHLIGHTS

- Cd, Pb, and Zn were still enriched in the final treated fly ash_3.
- External Hg, Cd, and Pb were captured in the fly ash_2.
- As^{5+} was removed after deacidification and slaked lime treatment.
- $HgSO_4$ and As^{3+} in the fly ash_3 was toxic and unstable.

GRAPHICAL ABSTRACT

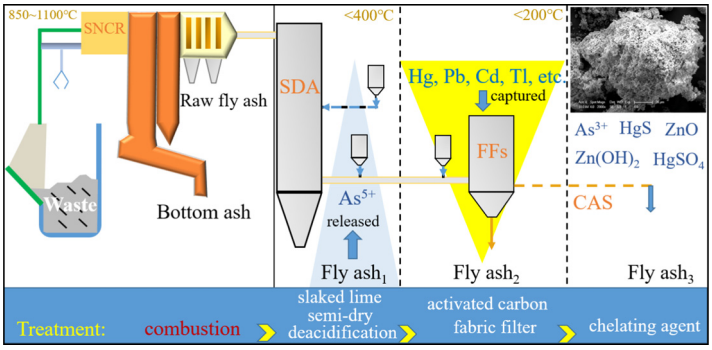

ARTICLE INFO

Article history:
Received 21 December 2021
Received in revised form 16 February 2022
Accepted 7 March 2022
Available online 15 March 2022

Editor: Daniel Alessi

Keywords:
Migration mechanism
Chemical speciation
Hazardous elements
Waste incineration plants

ABSTRACT

The transformation of heavy metals in ash from waste incineration plants is significant for ash management. The migration behavior of trace elements in ash after combustion, semidry deacidification, fabric filtration, and chelating agent stabilization was investigated from one waste incineration plant. The hazardous elements Zn, Pb, and As were enriched in raw fly ash (ash produced at a combustion temperature of 850–1100 °C) due to their relatively high volatility. Mercury, Cd, and Pb were captured in fly ash_2 and processed by activated carbon and fabric filters. The removal rate of As (71%) was the highest among all studied elements due to a large amount of quinquevalent As removed. However, the average removal rate of elements in fly ash was only 13%. In the finally obtained fly ash_3 (after chelating agent stabilization), a larger particle size (~100 μm) was found than that of raw ash. Furthermore, fly ash_3 contains $HgSO_4$ and trivalent As, which are toxic and likely to be precipitated when the fly ash_3 is next utilized or deposited in a landfill, causing environmental risks.

1. Introduction

Municipal solid waste (MSW) management is a significant issue that the modern world faces. This is especially true in developing countries where the amount of MSW has significantly increased due to rapid urbanization and industrialization. Global MSW is rising. Worldwide, cities produce 2.01 billion tonnes (t) of waste annually, which is predicted to rise to 3.4 billion t annually by 2050 (Kaza et al., 2018). As a populous developing country, China deserves special attention in this aspect. A major portion of MSW generated in China is attributed to organic components (61–95%), food waste (38–73%), plastics (2–14%), inorganic components (5–39%), and dirt and

* Corresponding author.
E-mail address: liuyuanm@ustc.edu.cn (Y. Liu).

http://dx.doi.org/10.1016/j.scitotenv.2022.154490

ash (0.2–36%) (Wang and Nie, 2009). Various methods, such as recycling, landfilling, and composting, have been used to manage MSW. Relevant national environmental protection standards were also issued to reduce the risks caused by domestic waste combustion, which outlined the fundamental requirements for MSW management: collection, storage, transportation, treatment, and disposal (Kanhar et al., 2020). Incineration is one of the most effective and widely used methods. Due to its effectiveness, incineration can remove up to 70% of waste by mass and 90% by volume. It can also breakdown hazardous components, nonmetallic organic wastes, and biological pollutants (Yu et al., 2013; Zhang et al., 2014). The presence of different inorganic contaminants, such as alkali metals, chlorine, sulfur, and heavy metals, is an unavoidable operational and environmental issue in waste incineration (Pedersen et al., 2009).

The main types of incineration technologies used for MSW in China are fluidized beds, stokers, and rotary kilns (Shi and Kan, 2009). Fluidized bed incinerators are widely used due to their remarkable ability to deal with MSW of low heat value. However, the production of byproducts, such as bottom ash, heat recovery ash, and pollution control residue, was two- to three-fold higher than that of the other technologies with the same incineration conditions (Yan et al., 2006). A previous study conducted in Switzerland revealed that incineration of one t household MSW produced up to 200 kg bottom ash, 22 kg gas cleaning residue, and 4 kg boiler ash (Belevi and Moench, 2000). In general, MSW incineration results in producing two types of ash: bottom ash and fly ash (Zhang et al., 2016). Bottom ash is the significant ash collected at the combustion chamber bottom. At the same time, fine particles filtered or captured from the flue gas with the help of air pollution control devices (scrubber) are called fly ash (Quina et al., 2018; U.S.EPA, 2014). These ash byproducts are complex mixtures of metals, salts, organic pollutants, and other components that might be toxic (Alorro et al., 2009). The content of metals in bottom ash and fly ash depends on the volatility of these metals. In general, bottom ash is rich in heavy metals with low volatility, mostly in the form of silicates. In contrast, fly ash is rich in volatile metals such as Zn, Ni, Cu, As, and Hg (Assi et al., 2020; Quina et al., 2018). These enriched hazardous elements can easily leach out of the ash, leading to soil and groundwater contamination and posing a severe risk to humans and the environment (Saqib and Bäckström, 2016).

To ensure proper disposal of potentially hazardous elements, it is essential to understand the basic physio-chemical properties, such as morphology, mineralogy, and chemical composition of ash produced by household waste combustion (Assi et al., 2020). Raw fly ash produced with high toxicity is often treated by activated carbon, slaked lime, and fabric filters for secure disposal (Jiang et al., 2007). However, few studies have investigated the speciation and mineralogical changes of hazardous trace elements in fly ash after successive treatment. Whether these treatments can effectively reduce the emission and mobility of trace elements remains to be studied. It is necessary to improve the effectiveness of existing waste incineration plants in terms of environmental safety. The present study aims to (1) estimate the concentrations of elements (Al, Ca, Fe, Mg, S, Si, As, Co, Cr, Cu, Mn, Ni, Pb, V, and Zn) in different ash samples at different stages of incineration and after chelating agent stabilization; (2) evaluate the enrichment behavior of trace elements detected in ash samples; and (3) use multiple techniques (namely, atomic fluorescence spectrophotometer (AFS), X-ray photoelectron spectroscopy (XPS), X-ray diffraction (XRD), and scanning electron microscopy with energy dispersive spectroscopy) for comprehensive characterization (physical and chemical) of elements in ash samples and to study their environmental behavior.

2. Materials and methods

2.1. Sample collection

The study was carried out in a household waste incineration plant with circulating fluidized bed boilers in Anhui, China. Samples of raw fly ash (ash produced due to combustion treatment at a temperature of 850–1100 °C), fly ash after semidry deacidification and the addition of slaked lime (fly ash_1), fly ash from the fabric filters, namely, fixed activated carbon filter (FACF) and fabric filter (FFs) (fly ash_2), fly ash after chelating agent stabilization (fly ash_3), bottom ash (combustion temperature of 850–1100 °C), activated carbon, and slaked lime were collected. A schematic sketch of the waste incineration plant is illustrated in Fig. 1. The basic information regarding the sampling plant and operating conditions is presented in Tables S1 and S2.

2.2. Element analysis

Powder samples (passed through 200 mesh sieve) of approximately 0.1 g were digested according to the previous method (Liu et al., 2016, 2018). Atomic Fluorescence Spectrophotometer (AFS-9130) was used to determine As, Hg, and Se. In contrast, Inductively-Coupled Plasma Mass Spectrometer (ICP-MS X Series II, Thermo Scientific, Bremen, Germany) was used to determine Be, Cd, Tl, U, and Sb. The rest of the elements (Al, Ca, Fe, Mg, S, Si, As, Co, Cr, Cu, Mn, Ni, Pb, V, and Zn) were analyzed using an Inductively Coupled Plasma-Optical Emission Spectrometer (ICP-OES, Perkin Elmer Optima, 2100DV).

To ensure quality control and data precision, certified reference material, NIST SRM 1633c was used for the coal fly ash. The recovery rates of the elements in the reference materials were in the range of 84.4% and 107.6%. The standard curves were linear ($R^2 > 0.99$, $n = 6$), indicating the accuracy and consistency of the analytical method. The instruments were tested with a standard solution (three times) after every tenth sample to ensure accuracy and stability. After analyzing blank samples and replicates, the relative standard deviation (RSD) was calculated, and the RSD value for all the detected elements was 0.07% ~ 18.5%.

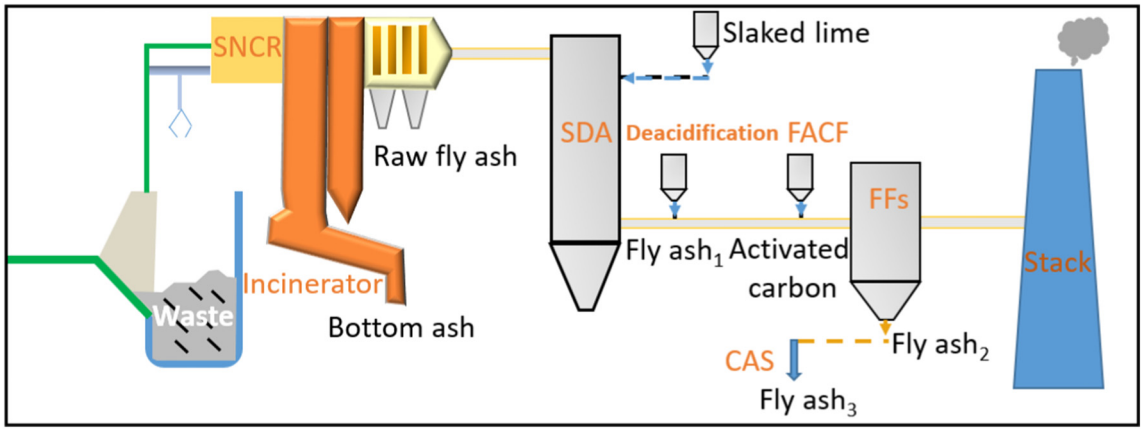

Fig. 1. Schematic of the waste incineration plant (SNCR, selective non-catalytic reduction; SDA, semidry absorber; FACF, fixed activated carbon filter; FFs, fabric filter; CAS, chelating agent stabilization).

2.3. X-ray photoelectron spectroscopy (XPS)

To determine the elements' surface chemistry and chemical form, ESCALAB 250 (Thermo-VG Scientific) was used. Monochromated Al K α X-ray source (1487 eV) at 150 kV, 20 Ma, at a selected area of 0.5 × 0.5 mm^2 was used to determine the overall composition, chemical state, and the spectra of particles were studied over >1100 eV at the resolution of 1 eV.

2.4. Scanning electron microscopy with energy dispersive spectroscopy (SEM/EDS)

SEM (ESEM, FEI Quanta 250 FEG), and EDS were used to determine the morphology and elemental composition. The method can provide qualitative semi-quantitative information with a resolution of 5× to 30,000×. To eliminate the effect of Al spectrum, the aluminum stubs were covered with adhesive tape, and the ash samples were positioned on the stubs for further analysis.

2.5. X-ray diffraction (XRD) analysis

To study the mineralogical content and physio-chemical properties of unknown materials in samples, XRD Rigaku D/max 2400 was used. It helps identify the size and shape of a unit cell within any compound. XRD technique was employed for phase identification, investigation of lattice parameters and phase fraction using Cu radiation at λ = 1.504 Å and scanning rate 8° min^{-1} from 20 to 80°. The diffraction patterns were used to find out the symmetry, size, and shape of particles and information of electron density which shows the position of the particles from peak intensities. Mineral phases in the samples were identified by XRD patterns using X'Pert High Score Plus software combined with the International Centre for Diffraction Data (ICDD) database.

2.6. Calculation

The enrichment factor (EF) was calculated to determine the partitioning behavior of trace elements among bottom ash, raw ash, fly ash_1, fly ash_2, and fly ash_3. After a sequential process, the removal rate was calculated to check the final removal rates of trace elements in the raw fly ash.

$$EF_1 = C_{raw\ fly\ ash}/C_{bottom\ ash} \quad (1)$$

$$EF_2 = C_{fly\ ash_1}/C_{raw\ fly\ ash} \quad (2)$$

$$EF_3 = C_{fly\ ash_2}/C_{fly\ ash_1} \quad (3)$$

$$EF_4 = C_{fly\ ash_3}/C_{fly\ ash_2} \quad (4)$$

$$\text{Removal rate}\ (\%) = \left(C_{raw\ fly\ ash} - C_{fly\ ash_3}\right)/C_{raw\ fly\ ash} \times 100 \quad (5)$$

where $C_{raw\ fly\ ash}$ is the concentration of trace elements in raw fly ash, $C_{bottom\ ash}$ is the concentration in bottom ash, $C_{fly\ ash_1}$ is the concentration in fly ash_1, $C_{fly\ ash_2}$ is the concentration in fly ash_2, and $C_{fly\ ash_3}$ is the concentration in fly ash_3.

3. Results and discussion

3.1. Trace element concentrations and distribution

The concentrations of elements detected in different ash samples collected from the waste incineration plant are presented in Table 1. Zinc was found to be the most dominant element in both bottom ash (3878 mg/kg) and raw fly ash (3557 mg/kg), followed by Pb (963 mg/kg) in raw fly ash and Cu (675 mg/kg) in bottom ash. Compared to the other samples, the concentrations of trace elements (Be, Co, Cr, Cu, Mn, Ni, and V) and major elements (Al, Fe, and Si) were highest in the bottom ash samples. In contrast, trace elements with higher volatility (As, Cd, Pb, Sb, Se, Tl, and Zn) were most enriched in raw fly ash. According to the results of EF_1, which showed the ratios of elements in the raw fly ash and bottom ash (Fig. 2), the EF_1 values of elements enriched in bottom ash were all lower than one, while the EF_1 values of elements enriched in raw fly ash were all higher than one. The distribution of elements in the different ash samples is dependent on two behaviors of the element, and these behaviors are based on the elements' volatility (Fernández et al., 1992; Wang et al., 2008). Nonvolatile elements always tend to form stable oxides and accumulate in coarser ash particles (Fu et al., 2018). Phongphiphat et al. (2011) showed that apart from Al, Fe, and Si, elements such as Ca, Mg, Zn, and Si were also found in bottom ash with high concentrations. Most of these elements have a high boiling point and are not volatile at low temperatures. They consequently ended up as part of the fly ash matrix.

Table 1
The concentrations of elements in the bottom ash, raw fly ash, fly ash_1, fly ash_2, fly ash_3, activated carbon, and slaked lime.

Elements	Unit	Bottom ash	Raw fly ash	Fly ash_1	Fly ash_2	Fly ash_3	Activated carbon	Slaked lime
Al	%	2.69	1.09	2.44	0.818	1.07	1.16	0.724
Ca	%	14.2	26.9	26.1	20.8	25.7	4.75	36.5
Fe	%	2.39	0.412	0.810	0.410	0.415	1.31	0.03
Mg	%	0.805	0.775	1.02	0.581	0.696	0.648	0.086
S	%	0.111	0.390	0.223	0.529	0.647	0.088	ND
Si	%	0.043	0.026	0.034	0.013	0.034	0.011	0.021
As	mg/kg	7.64	68.1	13.2	14.2	19.4	10.4	ND
Be	mg/kg	0.983	0.387	0.767	0.312	0.428	0.742	ND
Cd	mg/kg	6.92	210	43.8	149	165	8.47	ND
Co	mg/kg	14.9	5.04	7.20	3.60	3.36	7.92	ND
Cr	mg/kg	128	70.3	105	56.6	54.9	58.1	4.80
Cu	mg/kg	675	395	160	330	285	36.5	ND
Hg	mg/kg	0.693	6.27	1.07	14.1	5.95	1.38	ND
Mn	mg/kg	440	232	373	197	207	717	14.6
Ni	mg/kg	44.4	14.6	23.8	10.8	11.5	38.4	1.44
Pb	mg/kg	146	963	187	768	678	214	ND
Sb	mg/kg	0.869	3.82	1.85	1.53	2.02	0.792	0.182
Se	mg/kg	0.321	6.99	4.53	3.84	4.10	1.07	ND
Tl	mg/kg	0.042	1.10	0.260	0.836	0.929	0.382	ND
U	mg/kg	1.68	1.51	2.44	1.16	1.54	1.54	ND
V	mg/kg	20.2	6.48	15.6	4.80	5.52	15.8	ND
Zn	mg/kg	3557	3878	1831	2854	3012	1306	10.6

ND, not detected.

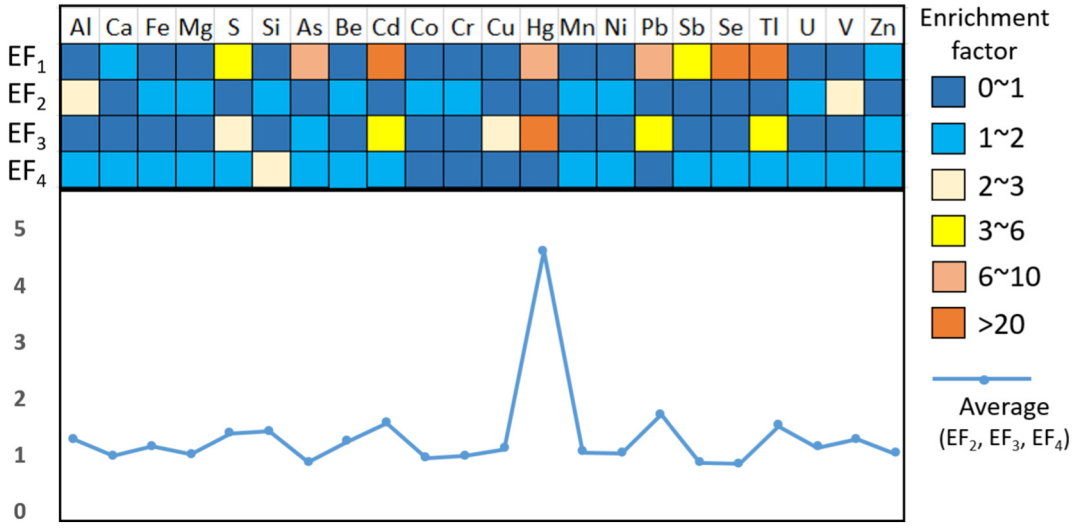

Fig. 2. Enrichment factors of trace elements among samples.

3.2. Migration behavior of trace elements in fly ash obtained during multiple incineration stages and treatment processes

3.2.1. Enrichment degree and influencing factors

The EF for trace elements in ash samples was calculated using Formulas (1)–(4) and is presented in Fig. 2 and Supplementary Table S3. The pH, operating temperature, and treatment process for each sample are listed in Table S2. The EF_1 values of highly volatile elements (As, Cd, Hg, Pb, Se, and Tl) were higher than six because these elements tend to be concentrated in raw fly ash. The results of EF_2, EF_3, and EF_4 showed the migration behavior of elements at different stages of incineration and after stabilizing the chelating agent. After each step of treatment, trace elements in ash changed considerably. The EF_2 values of Al, Fe, Mg, Si, Be, Co, Cr, Mn, Ni, U, and V were higher than one, indicating that the concentrations of these elements in fly ash_1 after being treated by deacidification and slaked lime at temperatures <400 °C were higher than those in raw fly ash. Among elements whose $EF_2 > 1$, no element had $EF_3 > 1$, indicating that no element concentration in fly ash continued to increase after being treated by activated carbon and fabric filter at temperatures <200 °C. However, among elements whose $EF_2 > 1$, Al, Fe, Mg, Si, Be, Mn, Ni, U, and V had $EF_4 > 1$, their concentrations continued to increase after treatment with CAS.

The comprehensive enrichment degree of the elements in fly ash during the above three steps could be observed through the average values of EF_2, EF_3, and EF_4. The average values of EF_2, EF_3, and EF_4 for Al, Fe, Mg, S, Si, Be, Cd, Cr, Cu, Hg, Mn, Ni, Pb, Tl, U, and V were higher than one, which means that these elements were enriched in treated fly ash. Mercury, Pb, and Cd had high average EF_2, EF_3, and EF_4 values. In addition, high concentrations of Hg (14.1 mg/kg), Pb (768 mg/kg), and Cd (149 mg/kg) were found in fly ash_2 (Table 1), indicating that during these steps (activated carbon + FACF + FFs), extra Hg, Cd, Pb from flue gas or other substances were trapped in fly ash_2. These chalcophile elements may be combined with S and captured by fly ash_2 together with S. The high S concentrations in fly ash_2 and fly ash_3 might be due to the sorption of sulfur oxides (such as SO_2) and condensation of volatilized species (such as metal sulfates) at moderately high temperatures. Sulfate species can be stable, particularly at temperatures below 800 °C (Poole, 2005; Verhulst et al., 1996).

Temperature and acid-base environments may affect the migration behavior of elements. During the treatment, the temperature continued to drop. Fly ash_1 was cooled from 850 °C ~ 1100 °C to <400 °C. The fly ash_1 treated with slaked lime presented alkalinity (pH = 11.77), the temperature of fly ash_2 decreased to <200 °C, and became weakly acidic (pH = 6.67), and the temperature of fly ash_3 continued to decline (Table S2). Mercury is associated with organic and inorganic matter and can evaporate totally during combustion. It cannot be detected mainly in the leachate, but it is believed that it reacts with the fly ash content and transforms to low exchangeable occurrences (Yudovich and Ketris, 2005). Cadmium may be vaporized to elemental form within the combustion zone (850–1100 °C). Through the downstream path of the flue gas, the elemental Cd can transform to $CdCl_2$ and $CdSO_4$ with decreasing temperature (Zhang et al., 2015). Lead can evaporate completely at a temperature of 600 °C to 1000 °C, and PbS is mainly predicted to be the most dominant species. The content of Pb was enriched at 1000 °C together with the formation of PbCl and PbO (Belevi and Moench, 2000). Most of the volatile elements were captured in the fly ash during flue gas transport downstream (Hower et al., 2013; Zhou et al., 2017).

3.2.2. Removal efficiency of the sequential process

The range of element removal rates in this study was −66% ~ 71%, and the average value was 13% (Table S3). Arsenic had the highest removal rate among all studied elements, reaching 71%, followed by Sb (47%) and Se (41%). Arsenic, Sb, and Se all had $EF_4 > 1$. They were not reduced after CAS treatment, which suggested two possibilities: (a) removal through a sequential process except CAS; (b) emission into the atmosphere in the form of gas or fine particles in the flue gas, which could impose a negative impact on the environment. Arsenic is mainly in vapor phase AsO (g) above 600 °C. However, upon decreasing the temperature below 500 °C, As is found in the condensed state (Zhang et al., 2015). The current study showed that the EF_2 of As was only 0.19, and the temperature of fly ash_1 dropped sharply, indicating that As in the raw fly ash may have been removed rather than evaporated. Activated carbon may be an essential additive for Sb and Se removal due to their EF_3 being lower than one. However, the adsorption capabilities are affected by various factors, such as the type of activated carbon, particle size, pH, and presence of salts, which might be the reasons for the low concentration of other elements (Tang and Steenari, 2016).

3.3. Chemical speciation of hazardous elements investigated by XPS analysis

The speciation of four volatile hazardous elements (Hg, As, Se, and Zn) enriched in fly ash was performed using XPS. The results are illustrated in Fig. 3. The XPS spectra for Hg show three dominant peaks at binding energies of 102.2 eV, 102.8 eV, and 103.4 eV in bottom ash, fly ash_1, and fly ash_3, attributed to HgS, $HgSO_4$, and $HgCl_2$, respectively. The curve fitting analysis of Hg referred to a previous study (Hao et al., 2018; Hutson et al., 2007). No Hg peaks were detected in the case of raw fly ash and fly ash_2. The results were similar in the case of As, for which no peaks were detected in fly ash_2. The difference is that As_2O_3 (44.1 eV), trivalent As (44.8 eV), and quinquevalent As (45.6 eV) were detected in raw fly ash. In the case of bottom ash, flyash$_1$, and fly ash_3, two dominant peaks for As_2O_3 and trivalent As were detected. These results matched previous studies (Ali et al., 2019; Fantauzzi et al.,

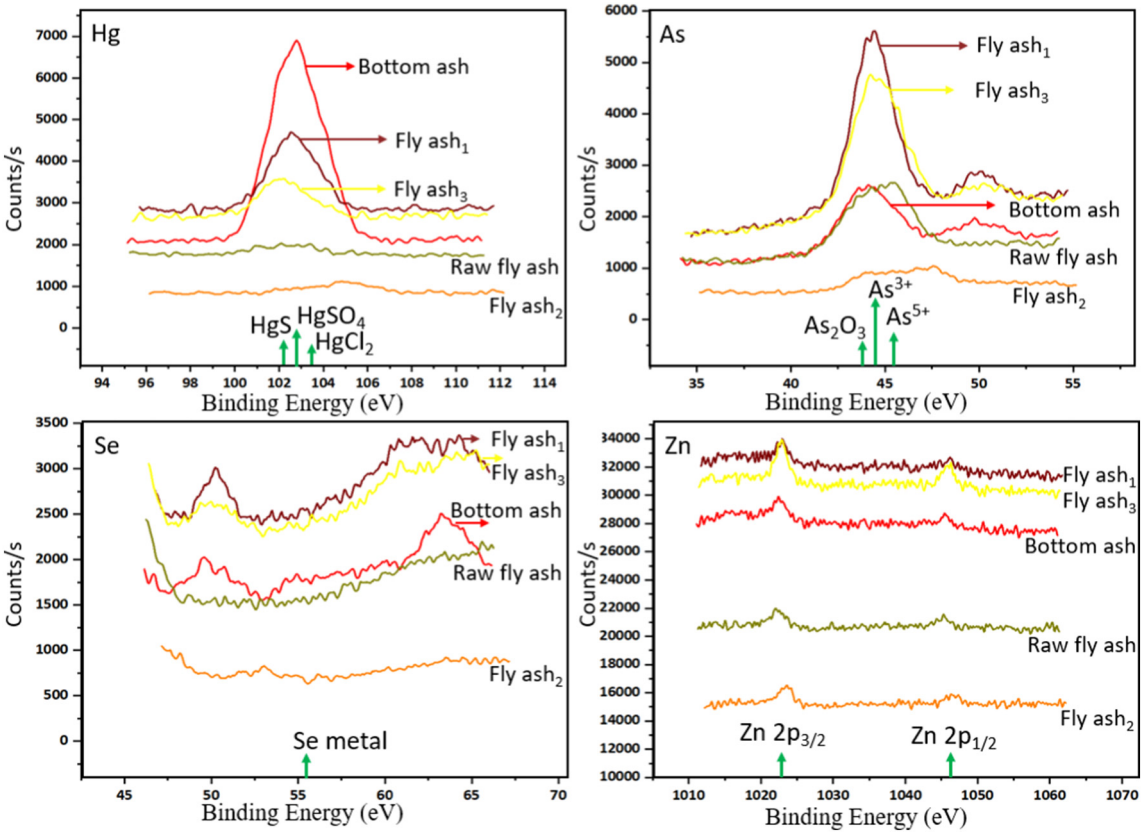

Fig. 3. The XPS spectra of Hg, As, Se, and Zn.

2006). In the case of Se, a single peak for metallic Se was detected in the bottom ash sample at a binding energy of 55.1 eV. The high-resolution XPS spectrum of the Zn $2p_{3/2}$ scan showed a dominant peak at a binding energy of approximately 1020 to 1024 eV, which refers to zinc oxide (ZnO) (1023.5 eV) and $Zn(OH)_2$ (1021 eV) (Şenadim Tüzemen et al., 2014; Winiarski et al., 2018). Another dominant peak was observed at 1045.1 eV, which is also attributed to ZnO and the natural form of metallic Zn. The trends for Zn were the same in all ash samples. The XPS spectra for C are presented in Supplementary Fig. S1. In the case of carbon, significant peaks for aliphatic CC and epoxy carbon (C-O-C) were detected at binding energies of 284.8 eV and 286 eV, respectively, in fly ash_1, fly ash_3, bottom ash, and raw fly ash. Another dominant peak at a binding energy of 288.5 eV was detected in all the ash samples that were carboxylate carbon (O-C=O) (Hellgren et al., 2016).

The effects of different treatment processes on the chemical speciation of elements in fly ash were further studied. Mercury in fly ash_1 treated after adding slaked lime mainly exists as $HgSO_4$. After deacidification and slaked lime treatment, unstable quinquevalent As in fly ash_1 was more effectively removed than the raw fly ash. After chelating agent treatment, fly ash_3 containing HgS, $HgSO_4$, and trivalent As, was likely to be precipitated again when the fly ash_3 was next utilized or deposited in a landfill, causing environmental risks (Liu et al., 2021).

3.4. Morphology of the ash obtained by different processes

The detailed morphology and major element composition of different ash samples were further investigated using SEM and EDS to reveal migration mechanisms. SEM images and detailed information for different ash samples are presented in Fig. 4 and Table S4. The SEM images of the ash were inhomogeneous with a variety of needle, spherical, blocky, and irregular structures with a size range of 1 to 100 μm. Fig. 4 (A) demonstrates the SEM image for the bottom ash sample. Different types of structures were observed in the bottom ash, while there was no proper indication of the surface and interior of the particles. Most of the particles were spherical or blocky. It appeared that spherical particles were formed due to high temperature and looked like molten materials with smooth spheres, while the irregular geometry may be attributed to low combustion temperatures (Phongphiphat et al., 2011; Saikia et al., 2006). The content of elements in the bottom ash was very high, especially in the case of Ca, Fe, Mg, Ti, Zr, Cr, and Si. Calcium was the most dominant element along with Si, and both of these elements are the typical elements found in combustion residue (Wang et al., 2008). The high Ca content in the bottom ash might be attributed to the presence of calcium carbonate and calcium sulfate ($CaSO_4$). The presence of Na and K might be attributed to sodium chloride and potassium dioxide (Chen and Chiou, 2007; Jiang et al., 2007).

An SEM image of the raw fly ash sample is shown in Fig. 4 (B, F). The EDS results for raw fly ash show a variety of elements, such as Na, Si, Cl, K, Cr, Ca, Co, Ni, Pt, and Zn, to be the most dominant. In contrast, the presence of Cl and alkali metals may be attributed to the condensation of alkali chlorides of the fly ash, especially during the entry phase into the exhaust gas. Apart from that, a high content of C was detected during EDS analysis, which might indicate unburned materials (Rodella et al., 2016; Yu et al., 2013). The predominant elements in fly ash_1 (Fig. 4 C) were oxygen (O), Si, C, Al, and Cr. It is believed that due to the high solubility of alkali and earth metal chlorides, most of the elements might be removed during deacidification. The particle size for fly ash_1 varied from submicron up to 100 μm and was dominated mainly by plate-structured particles. Fly ash_2, which has higher adhesion between particles, was mainly below 100 μm, with very few large particles (Fig. 4 D). A variety of porous, small, and irregularly shaped particles were detected. The most dominant elements in fly ash_2 were C, O, Cl, Ca, and Pt. The SEM and EDS results for fly ash_2 samples show agglomeration of finer particles. These results might indicate the presence of potassium (K). Potassium can react with other alkali metals to form sticky alkali metal compounds such as sulfates and start bonding as vapors condense on cooler surfaces, leading to the accumulation of particles through impaction (Jiménez and Ballester, 2005; Walser et al., 2012). Fly

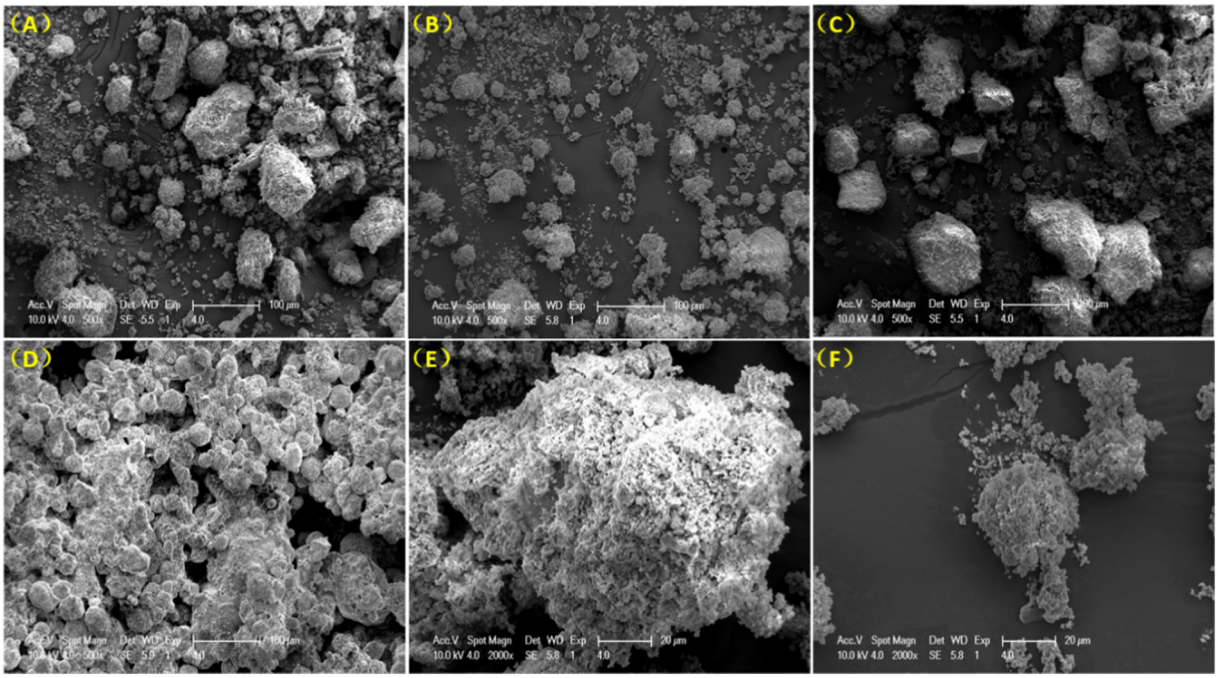

Fig. 4. SEM images of samples. (A) Bottom ash (500×), (B) raw fly ash (500×), (C) fly ash_1 (500×), (D) fly ash_2 (500×), (E) fly ash_3 (2000×), and (F) raw fly ash (2000×).

ash_3 became substantially larger than raw fly ash after being treated with a chelating agent. A blocky and irregular appearance was observed, with O, Mg, Si, and Ca being the most dominant particles (Fig. 4 E).

3.5. The difference in mineral composition

The mineralogical composition of municipal waste ash was studied using XRD. Combining the XRD results with SEM can further reveal the minerals that might be present in each ash, thus revealing the possible trace element alien minerals. The XRD spectra for different ash samples are presented in Fig. 5. The XRD pattern for the bottom ash shows that the major crystalline phase was attributed to quartz (SiO_2) (d-spacing 3.33 and 3.03), which is also consistent with the SEM results. Apart from that, small peaks for calcite, calcium carbonate, and anhydrite were also observed. The results were consistent with those previously presented by Yu et al. (2013). In the case of raw fly ash, the XRD pattern was dominated by halite and fluorite. Apart from these, minor stannite, coesite, and potassium sodium chloride concentrations were also observed. The fly ash_1 samples were dominated by calcite, uraninite, and fluorite, while in fly ash_2 and fly ash_3, halite, and calcite were dominant. Overall, the major crystalline phase in fly ash samples was dominated by $CaCO_3$, SiO_2, $CaSO_4$, and NaCl, and these results were found to be consistent with previous pieces

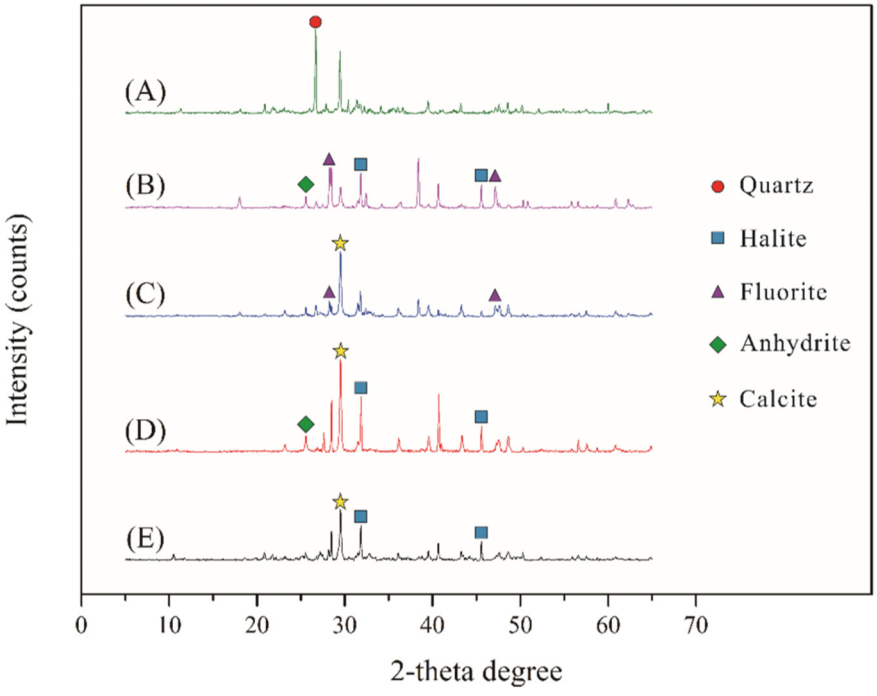

Fig. 5. Mineral composition of the samples. (A) Bottom ash, (B) raw fly ash, (C) fly ash_1, (D) fly ash_2, (E) fly ash_3.

of literature (Fedje et al., 2010; Jung et al., 2004). The mineralogical content of fly ash samples is highly dependent on temperature, waste composition, gas velocity, and the type of furnace used (Chang et al., 2009).

4. Conclusion

Attention was given to the influence of the different technical processes on the transformation of trace elements in ash from waste incineration plants in this study. The main factors affecting hazardous element migration in fly ash were treatment technology and temperature, based on observations made using XRD and SEM: (a) After slaked lime treatment, the main mineral components in fly ashes became calcite; (b) ash samples were inhomogeneous with a variety of needle, spherical, blocky and irregular structures that may be attributed to the condensation of volatile compounds during the process.

Bottom ash and raw fly ash were directly generated by combustion. The high concentrations of many elements in bottom ash might be due to their high boiling points and low volatility, while the high concentrations of elements such as Pb, Cd, and As in raw fly ash may be attributed to their high volatility, which also highlights the importance of temperature in the behavior of these elements. Some volatile elements were captured by fly ash during the sequential process, and some were removed. There was a high chance for elements such as Hg, Cd, and Pb from flue gas captured in the fly ash_2. The high proportion of As, Sb, and Se in the fly ash was removed during the sequential process; however, the average removal rate through the sequential process was just 13%, Cd, Pb, and Zn were still enriched in the final treated fly ash_3. In addition, toxic $HgSO_4$ and trivalent As observed in the final fly ash_3, threaten the surrounding environment. Thus, special treatment or sorting management should be strengthened for waste that is rich in these elements.

CRediT authorship contribution statement

Muhammad Ubaid Ali: Writing- Original draft preparation, Conceptualization, Methodology, Software, Funding acquisition, Data curation; **Yuan Liu:** Conceptualization, Funding acquisition, Validation, Visualization, Writing - Review & Editing; **Balal Yousaf:** Methodology; **Ming Hung Wong**: Review & Editing; **Ping Li:** Software, Data curation, Funding acquisition; **Guijian Liu:** Review & Editing; **Ruwei Wang:** Investigation, Formal analysis, Software; **Yong Wei:** Methodology, Supervision, Investigation; **Muyuan Lu:** modification.

Declaration of competing interest

The authors declare that they have no known competing financial interests or personal relationships that could have appeared to influence the work reported in this paper.

Acknowledgment

This work was supported by the National Natural Science Foundation of China (Nos. 41902163, and 41773099), the Anhui Provincial Natural Science Foundation (1908085QD154).

Appendix A. Supplementary data

Supplementary data to this article can be found online at https://doi.org/10.1016/j.scitotenv.2022.154490.

References

Ali, M.U., Liu, G., Yousaf, B., Ullah, H., Irshad, S., Ahmed, R., Hussain, M., Rashid, A., 2019. Evaluation of floor-wise pollution status and deposition behavior of potentially toxic elements and nanoparticles in air conditioner dust during urbanistic development. J. Hazard. Mater. 365. https://doi.org/10.1016/j.jhazmat.2018.11.005.

Alorro, R.D., Hiroyoshi, N., Ito, M., Tsunekawa, M., 2009. Recovery of heavy metals from MSW molten fly ash by CIP method. Hydrometallurgy 97, 8–14.

Assi, A., Bilo, F., Zanoletti, A., Ponti, J., Valsesia, A., La Spina, R., Zacco, A., Bontempi, E., 2020. Zero-waste approach in municipal solid waste incineration: reuse of bottom ash to stabilize fly ash. J. Clean. Prod. 245, 118779. https://doi.org/10.1016/j.jclepro.2019.118779.

Belevi, H., Moench, H., 2000. Factors determining the element behavior in municipal solid waste incinerators. 1. Field studies. Environ. Sci. Technol. 34, 2501–2506.

Chang, C., Wang, C., Mui, D.T., Cheng, M., Chiang, H., 2009. Characteristics of elements in waste ashes from a solid waste incinerator in Taiwan. J. Hazard. Mater. 165, 766–773. https://doi.org/10.1016/j.jhazmat.2008.10.059.

Chen, C.H., Chiou, I.J., 2007. Distribution of chloride ion in MSWI bottom ash and dechlorination performance. J. Hazard. Mater. 148, 346–352.

Fantauzzi, M., Atzei, D., Elsener, B., Lattanzi, P., Rossi, A., 2006. XPS and XAES analysis of copper, arsenic and sulfur chemical state in enargites. Surf. Interface Anal. 38, 1380–1385. https://doi.org/10.1002/sia.

Fedje, K.K., Rauch, S., Cho, P., Steenari, B., 2010. Element associations in ash from waste combustion in fluidized bed. Waste Manag. 30, 1273–1279. https://doi.org/10.1016/j.wasman.2009.09.012.

Fernández, M.A., Martínez, L., Segarra, M., Garcia, J.C., Espiell, F., 1992. Behavior of trace imuniciple waste incineration using (circulating fluidized bed boilers) properties. Environ. Sci. Technol 26, 1040–1047.

Fu, B., Liu, G., Sun, M., Hower, J.C., Mian, M.M., Wu, D., Wang, R.W., Hu, G.Q., 2018. Emission and transformation behavior of minerals and hazardous trace elements (HTEs) during coal combustion in a circulating fluidized bed boiler. Environ. Pollut. 242, 1950–1960. https://doi.org/10.1016/j.envpol.2018.07.066.

Hao, R., Yang, F., Mao, X., Mao, Y., Zhao, Y., Lu, Y., 2018. Emission factors of mercury and particulate matters, and in situ control of mercury during the co-combustion of anthracite and dried sawdust sludge. Fuel 230, 202–210.

Hellgren, N., Haasch, R.T., Schmidt, S., Hultman, L., Petrov, I., 2016. Interpretation of X-ray photoelectron spectra of carbon-nitride thin films: new insights from in situ XPS. Carbon N.Y. 108, 242–252. https://doi.org/10.1016/j.carbon.2016.07.017.

Hower, J.C., O'Keefe, J.M.K., Henke, K.R., Wagner, N.J., Copley, G., Blake, D.R., Garrison, T., Oliveira, M.L.S., Kautzmann, R.M., Silva, L.F.O., 2013. Gaseous emissions and sublimates from the Truman shepherd coal fire, Floyd county J., Kentucky: a re-investigation following attempted mitigation of the fire. Int. Coal Geol. 116–117, 63–74.

Hutson, N.D., Attwood, B.C., Scheckel, K.G., 2007. XAS and XPS characterization of mercury binding on brominated activated carbon. Environ. Sci. Technol 41, 1747–1752.

Jiang, J.G., Xu, X., Wang, J., Yang, S.J., Zhang, Y., 2007. Investigation of basic properties of fly ash from urban waste incinerators in China. J. Environ. Sci. 19, 458–463. https://doi.org/10.1016/S1001-0742(07)60076-X.

Jiménez, S., Ballester, J., 2005. Influence of operating conditions and the role of sulfur in the formation of aerosols from biomass combustion. Combust. Flame 140 346–35.

Jung, C.H., Matsuto, T., Tanaka, N., Okada, T., 2004. Metal distribution in incineration residues of municipal solid waste (MSW) in Japan. Waste Manag. 24, 381–391. https://doi.org/10.1016/S0956-053X(03)00137-5.

Kanhar, A.H., Chen, S., Wang, F., 2020. Incineration fly ash and its treatment to possible utilization: a review. Energies 13 (24), 6681. https://doi.org/10.3390/en13246681.

Kaza, S., Yao, L., Bhada-Tata, P., Van Woerden, F., 2018. What a Waste 2.0: A Global Snapshot of Solid Waste Management to 2050. Urban Development Series. World Bank, Washington, DC. https://doi.org/10.1596/978-1-4648-1329-0 License: Creative Commons Attribution CC BY 3.0 IGO.

Liu, Y., Liu, G., Qi, C., Cheng, S., Sun, R., 2016. Chemical speciation and combustion behavior of chromium (Cr) and vanadium (V) in coals. Fuel 184, 42–49.

Liu, Y., Liu, G., Yuan, Z., Liu, H., Lam, P.K.S., 2018. Heavy metals (As, hg and V) and stable isotope ratios (δ13C and δ15N) in fish from Yellow River Estuary, China. Sci. Total Environ. 613–614, 462–471.

Liu, Y., Liu, G., Yousaf, B., Zhou, C., Shen, X., 2021. Identifcation of the featured-element in fine road dust of cities with coal contamination by geochemical investigation and isotopic monitoring. Environ. Int. 152, 106499.

Pedersen, A.J., Frandsen, F.J., Riber, C., Astrup, T., Thomsen, S.N., Lundtorp, K., Mortensen, L.F., 2009. A full-scale study on the partitioning of trace elements in municipal solid waste incinerations-effects of firing different waste types. Energy Fuels 23, 3475–3489. https://doi.org/10.1021/ef801030p.

Phongphiphat, A., Ryu, C., Finney, K.N., Sharifi, V.N., Swithenbank, J., 2011. Ash deposit characterisation in a large-scale municipal waste-to-energy incineration plant. J. Hazard. Mater. 186, 218–226. https://doi.org/10.1016/j.jhazmat.2010.10.095.

Poole, D.J., 2005. Identification and Control of Metal Pollutant Spikes in Municipal Solid Waste Incinerators. University of Sheffield, Sheffield, UK PhD Thesis.

Quina, M.J., Bontempi, E., Bogush, A., Schlumberger, S., Weibel, G., Braga, R., Funari, V., Hyks, J., Rasmussen, E., Lederer, J., 2018. Technologies for the management of MSW incineration ashes from gas cleaning: new perspectives on recovery of secondary raw materials and circular economy. Sci. Total Environ. 635, 526–542. https://doi.org/10.1016/J.SCITOTENV.2018.04.150.

Rodella, N., Pasquali, M., Zacco, A., Bilo, F., Borgese, L., Bontempi, N., Tomasoni, G., Depero, L.E., Bontempi, E., 2016. Beyond waste: new sustainable fillers from fly ashes stabilization, obtained by low cost raw materials. Heliyon 2.

Saikia, N., Kato, S., Kojima, T., 2006. Compositions and leaching behaviours of combustion residues. Fuel 85, 264–271.

Saqib, N., Bäckström, M., 2016. Chemical association and mobility of trace elements in 13 different fuel incineration fly ashes. Fuel 165, 193–204. https://doi.org/10.1016/j.fuel.2015.10.062.

Şenadim Tüzemen, E., Şahin, H., Kara, K., Elagöz, S., Esen, R., 2014. XRD, XPS, and optical characterizations of Al-doped ZnO film grown on GaAs substrate. Turk.J. Phys. 38, 111–117. https://doi.org/10.3906/fiz-1301-17.

Shi, H.S., Kan, L.L., 2009. Leaching behavior of heavy metals from municipal solid wastes incineration (MSWI) fly ash used in concrete. J. Hazard. Mater. 164 (2), 750–754.
Tang, J., Steenari, B.M., 2016. Leaching optimization of municipal solid waste incineration ash for resource recovery: a case study of Cu, Zn, Pb and Cd. Waste Manag. 48, 315–322. https://doi.org/10.1016/j.wasman.2015.10.003.
U.S.EPA, 2014. Municipal Solid Waste Basic Information. PhD Thesis http://www.epa.gov/epawaste/nonhaz/municipal/wte/basic.htm.
Verhulst, D., Buekens, A., Spencer, P.J., Eriksson, G., 1996. Thermodynamic behavior of metal chlorides and sulfates under the conditions of incineration furnaces. Environ. Sci. Technol. 30, 50–56.
Walser, T., Limbach, L.K., Brogioli, R., Erismann, E., Flamigni, L., Hattendorf, B., Juchli, M., Krumeich, F., Ludwig, C., Prikopsky, K., Rossier, M., Saner, D., Sigg, A., Hellweg, S., Günther, D., Stark, W.J., 2012. Persistence of engineered nanoparticles in a municipal solid-waste incineration plant. Nat. Nanotechnol. 7, 520–524. https://doi.org/10.1038/nnano.2012.64.
Wang, H., Nie, Y., 2009. Municipal solid waste characteristics and management in China. J. Air Waste Manag. Assoc. 6, 173–180.
Wang, S., Baxter, L., Fonseca, F., 2008. Biomass fly ash inn concrete: SEM, EDX and ESEM analysis. Fuel 87, 372–379.
Winiarski, J., Tylus, W., Winiarska, K., Szczygieł, I., Szczygieł, B., 2018. XPS and FT-IR characterization of selected synthetic corrosion products of zinc expected in neutral environment containing chloride ions. J. Spectrosc. 2018. https://doi.org/10.1155/2018/2079278.
Yan, J., Chen, T., Li, X., Zhang, J., Lu, S., Ni, M., Cen, K., 2006. Evaluation of PCDD/Fs emission from fluidized bed incinerators co-firing MSW with coal in China. J. Hazard. Mater. 135 (1), 47–51.
Yu, J., Sun, L., Xiang, J., Jin, L., Hu, S., Su, S., Qiu, J., 2013. Physical and chemical characterization of ashes from a municipal solid waste incinerator in China. Waste Manag. Res. 31, 663–673. https://doi.org/10.1177/0734242X13485793.
Yudovich, Y., Ketris, M.P., 2005. Mercury in coal : a review part 1. Geochemistry. Int. J. Coal Geol. 62, 107–134.
Zhang, L., Su, X., Zhang, Z., Liu, S., Xiao, Y., Sun, M., Su, J., 2014. Characterization of fly ash from a circulating fluidized bed incinerator of municipal solid waste. Environ. Sci. Pollut. Res. 21, 12767–12779. https://doi.org/10.1007/s11356-014-3241-9.
Zhang, Y., Nakano, J., Liu, L., Wang, X., Zhang, Z., 2015. Trace element partitioning behavior of coal gangue-fired CFB plant: experimental and equilibrium calculation. Environ. Sci. Pollut. Res. 22, 15469–15478. https://doi.org/10.1007/s11356-015-4738-6.
Zhang, Y., Chen, J., Likos, W.J., Edil, T.B., 2016. Leaching characteristics of trace elements from municipal solid waste incineration fly ash. Geo-Chicago 2016 GSP. 273, pp. 168–178. https://doi.org/10.1061/9780784480168.018 License: Creative Commons Attribution CC BY 3.0 IGO.
Zhou, C., Liu, G., Xu, Z., Sun, H., Lam, P.K.S., 2017. The retention mechanism, transformation behavior and environmental implication of trace element during co-combustion coal gangue with soybean stalk. Fuel 189, 32–38. https://doi.org/10.1016/j.fuel.2016.10.093.